

SOLID PROPELLANT MICRO-ROCKETS – TOWARDS A NEW TYPE OF POWER MEMS

B. Larangot¹, C. Rossi¹, T. Camps¹, A. Berthold¹
P.Q. Pham², D. Briand², N.F. de Rooij²
M. Puig-Vidal³, P. Miribel³, E. Montané³, E. López³, J. Samitier³

¹ LAAS-CNRS, 7 ave du colonel Roche, 31077 Toulouse cedex 4, France

² IMT, University of Neuchâtel, Jaquet-Droz 1, P.O. Box 3, CH-2007 Neuchâtel, Switzerland

³ Instrumentation & Communication Systems (SIC), c/ Martí Franquès 1, 08028 Barcelona, Spain

Abstract

The paper presents a new type of power MEMS, called solid propellant micro-rocket or thruster. It is based on the integration of a propellant within a silicon micromachined system. The operational concept is simply based on the combustion of an energetic propellant stored in a micromachined chamber. Each rocket contains three parts (heater, chamber, nozzle) and has no channels or valves. Due to the one shot characteristic, micro-rockets are fabricated in array configuration. One field of application is micropropulsion for nanosatellite or actuation of power units. This paper details the design, fabrication and testing of arrays of solid propellant rockets assembled with the electronics needed for communicating, addressing and powering. Rockets presented in this paper feature chamber section of equal 2.25mm². Throat diameter is either 105µm or 150µm. The heater sizes ranges from 540µm×540µm to 720µm×720µm. First characterizations gave ignition energy of hundred mJ and resulting impulse bit force of a few mN.s. The paper also presents a new type of rocket device and new energetic material under investigation for application requiring very small and precise impulse (below the mN.s).

I. Introduction

Different types of combustors or rockets engines have been published [1-4]. They face major technological difficulties due to the complexity of these devices and present relatively low efficiency caused by energy losses by friction. Solid propellant micro-rocket concept is simple and has no moving parts offering two main advantages :

- The frictional forces inherent to moving parts are eliminated.
- There is no liquid fuel, no leakage possible can take place and the propellant remains stable over time.

The most obvious application of these micro-rockets is the micropropulsion for space. Depending on the

mass of the nanospacecraft, solid propellant micro-rockets can achieve velocity increments ranging from 0.6×10⁻³ m/s to 20m/s [5]. Other applications have also been identified as actuation of power units, gas generation device to release some mechanical panels or parts

The paper describes the design of a millimeter scale micro-rocket and gives initial results obtained for the fabrication, assembling and testing. The challenges in making solid propellant rocket can be divided into the fundamental physical difficulties and the engineering issues. The fundamental physical difficulties will be presented in a second paper [6]. In the second category, many engineering difficulties are evident and will be reviewed in this paper :

- the compromise between the reduction of the dimensional features and combustion process consideration.
- the interfacing, interconnection and packaging of the systems, the 2D addressing design and realization.
- the management in a very small volume of high temperature and high pressure that could lead to mechanical failures,
- the limits of silicon and the introduction of best appropriate material implying to bond different materials.
- the use of propellant material that is limitative for micro scale devices leading us to reconsider explosive and structure geometry for more compact devices.

II. Design & layout

II.1 The micro-rocket structure

Figure 1 gives a schematic view of one single rocket. It consists of 4 parts of silicon :

- A silicon micromachined igniter with a polysilicon resistor patterned onto a very thin dielectric membrane.
- A propellant reservoir which defines the combustion chamber.

- A nozzle wafer added on the top of the structure.
- A seal wafer.

Chambers are fabricated using Foturan or silicon and the nozzle and igniter parts are realized by micro machining the silicon.

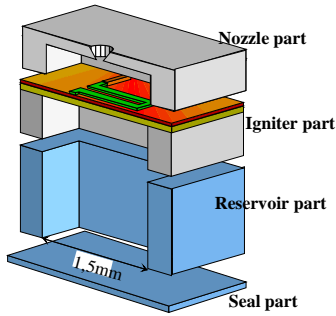


Figure 1: Schematic view of one single micro-rocket.

The dimensions of individual rockets are in the millimeter scale for the chamber and in the micrometer scale for the nozzle. Dimensions could seem large for a MEMS device and especially when a high density of integration is desired. However, limitations on the scaling down the device appeared due to the thermal crosstalk [6] and combustion considerations. Two main issues have been taken into consideration for design:

- Used propellant material doesn't have sustained combustion for a combustion section below 1.8mm^2 when the propellant is surrounded with glass (discussed in §IV.2). Indeed the combustion of propellant is a competition between the thermal loss through the structure wall and the rate of heat produced by the combustion. When the thermal crosstalk become greater than heat produced, the combustion stops.
- For nanosat StationKeeping or nanosat de orbit application, first evaluations of the thrust and total impulse [5] lead us to design rocket having chamber section over the mm^2 .

As shown in Figure 2 and Table 1, the chamber lateral dimension is fixed at 1.5mm ; throat diameter (Φ_t) is either $150\mu\text{m}$ or $105\mu\text{m}$ depending on the desired combustion pressure; chamber length (H_1+H_2) is 1.5mm . Two chamber pressure points are expected: one below 20Bars and one above 30Bars .

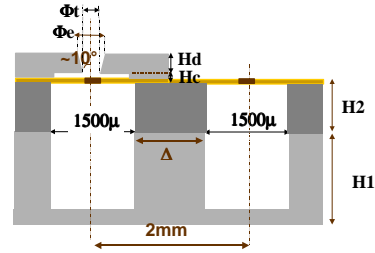


Figure 2: Geometrical characteristics of rockets array.

Φ_c	$150\mu\text{m}$	
Φ_t	$150\mu\text{m}$	$105\mu\text{m}$
Φ_e	$170\mu\text{m}$	$120\mu\text{m}$
A_c/A_t	100	204
Predicted combustion pressure	14bars	35bars
H_c	Few hundreds μm	
H_d	$60\mu\text{m}$	$50\mu\text{m}$
H_2	$350\mu\text{m}$	
H_1	1mm	
Δ	$500\mu\text{m}$	

Table 1: Dimensions.

II.2 The 2D addressed array principle

The final array contains 100 separate micro-rockets on $24\text{mm} \times 24\text{mm}$ silicon chip. The interconnection techniques and assembling procedures are strongly related to the electronic system architecture definition compatible to microsystem assembling. Each rocket could be addressed independently on the order of a computer. The addressing is realized by placing PN junction in series with the heater filament as shown in Figure 3.

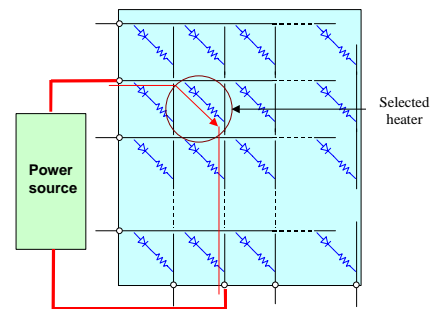


Figure 3: Schematic view of a 2D addressed matrix of resistors.

The PN junctions have been designed to pass 500mW through a resistor of 1kohm with a maximum current of 30mA. We optimized the process (implantation and annealing parameters) and the design to obtain a breakdown voltage higher than 40 V and to minimize the forward voltage ($>2V$; $I = 23 \text{ mA}$). ATHENA simulations of our optimized structure give the doping profile as shown in Figure 4.

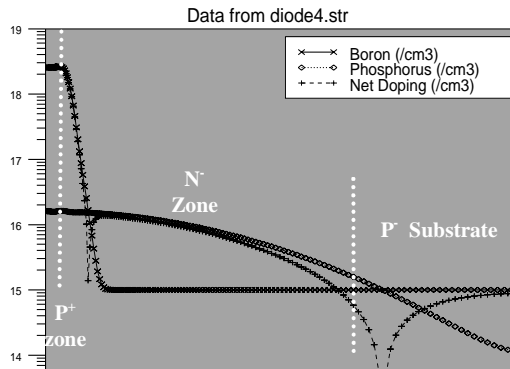


Figure 4: Simulated doping profile of the PN Junction.

II.3 The electronic chip design

In order to develop the electronic circuitry needed for our specific application some considerations have to be taken into account:

- The electronic circuitry has to contribute to optimize the ignition process.
- A safety condition must be ensured, avoiding uncontrolled ignitions.
- A wireless autonomous system using a battery based power delivery system and RF communication module is needed for the application.

The proposed electronic system architecture is based on six main blocs connected to a data bus (Figure 5).

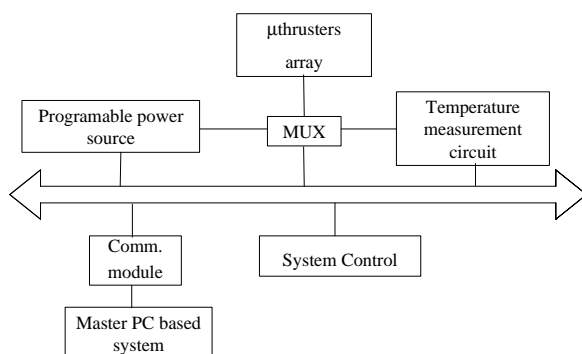


Figure 5: Electronic system architecture.

Different control functions necessary for the ignition optimization and test have been implemented in a Digital Control system. Some examples of main control functions included are:

- Resistance and Temperature measurement,
- Preheating of a micro-rocket to achieve a specific temperature before ignition
- Preheating of a micro-rocket to achieve a specific temperature condition on-line, with temperature measurement of the selected micro-rocket and its neighbors during the heating process.

A platform test using first discrete implementation of proposed electronic system architecture has been performed (Figure 6). The control functions previously described are implemented in a FPGA based Digital Control system. This test platform will contribute to improve and validate the control algorithms and the optimization of the ignition process.



Figure 6: First discrete implementation of proposed electronic system architecture: analog and digital control system circuitry in the left side and connected first 4x4 micro-rockets array in the right side.

For the validation and test of the micro-rocket array, microelectronic Integrated Circuit technologies will be used to integrate all this circuitry in the minimum silicon area. In order to integrate this proposed electronic system architecture in the backside of the microthuster array ($28 \times 28 \text{ mm}^2$) specific technologies I2T100 (ALCATEL Microelectronics) and AMS 0.35mm (Austria Mycro Systems) have been used. Different ICs will be implemented to be assembled in the backside of micro-rocket array. Microelectronic Integrated Circuit design tools for Hardware/Software Codesign will be used for this purpose.

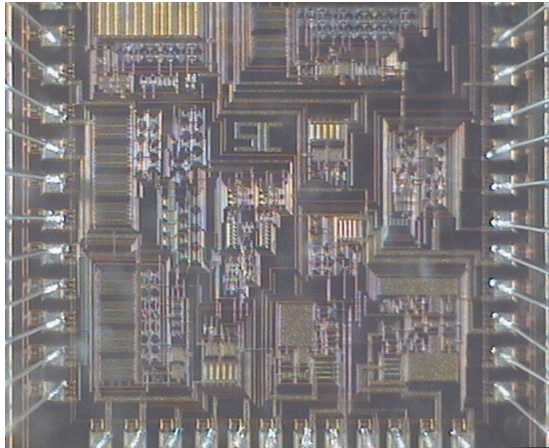


Figure 7: Integrated Circuit, implemented in I2T100 technology from ALCATEL, including a DC-to-DC converter as a programmable power source and Multiplexer system (MUX) to address power to the specific micro-rocket.

A first Integrated Circuit has been already designed in I2T100 technology containing a DC-to-DC converter as a programmable power source and Multiplexer system (MUX) to address power to the specific microthuster (Figure 7). The I2T100 technology from Alcatel is a DMOS-BiCMOS technology with voltage capabilities up to 100 V. The power system designed includes a voltage to current source based on a window comparator [7] and a Multiplexer system to address the current output to the selected micro-rocket in the microsystem array. A constant current is sourced to the micro-rocket resistance during the heating process and the temperature evolution is obtained by measuring the voltage drop across this resistance.

III. Processing

III.1 Igniters wafer

III.1.1 Fabrication of the heater filament

A 350 μm thick (100) oriented silicon wafer is thermally oxidized. Then, the wafers are coated with silicon rich LPCVD (Low Pressure Chemical Vapor Deposition) nitride. The resulting thickness is 2 μm . In a third step, a layer of 0.5 μm of polysilicon is deposited by LPCVD at 605 $^{\circ}\text{C}$ and doped by diffusion. The heater filament is patterned using a reactive ion etching (RIE). Then, the electrical pads and electrical supply lines are realized in gold. To realize the membrane, the silicon is etched away by Deep Reactive Ion Etching (DRIE). Arrays of 16 non-addressed heaters have been realized to characterize the propellant ignition (cf. Figure 8).

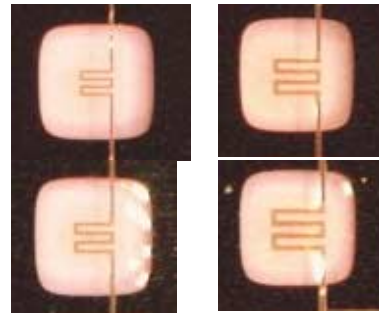
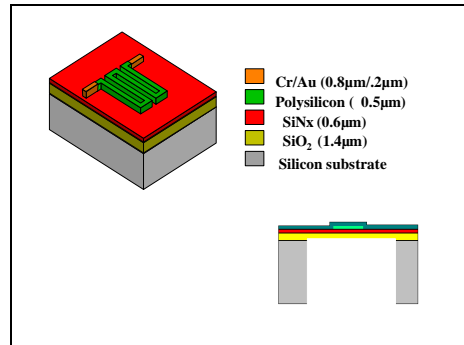


Figure 8: Schematic view of a single silicon micro machined igniter and photos of different sizes of heater filaments on dielectric membrane.

III.1.2 Fabrication of the 2D addressed arrays

The first realisation of micro-rockets array (10 \times 10) is shown in Figure 9. We ensure the compatibility between micro-rockets fabrication and PN junction process (8 masks levels). For next realisation the diode area will be reduced from 2.10 $^{-4}$ to 4.10 $^{-5}$ cm 2 .

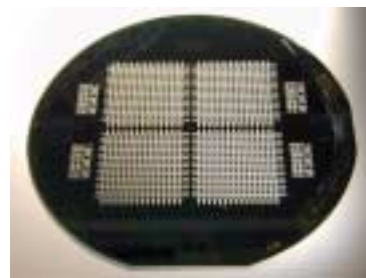


Figure 9: Photos of 10 \times 10 micro heaters addressed arrays.

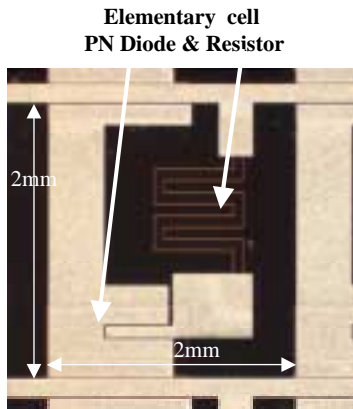


Figure 10: Photo of an elementary cell (diode + resistor).

The I(V) characteristic of fabricated PN junction is shown in Figure 11. We obtained a 45V breakdown voltage and 1.5V for a forward current $I = 30$ mA.

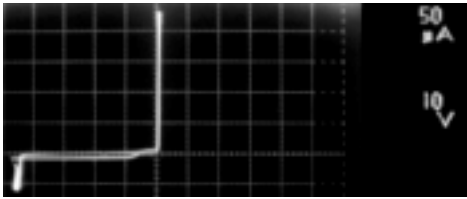


Figure 11: I(V) characteristic of a PN Junction.

III.2 Fabrication of the nozzle wafer

The nozzle is mainly composed of two elements: a throat and a diverging part (Figure 12). The divergent angle α has been set to 10° . The nozzles are fabricated by DRIE and their process is still under development. In order to form the divergent angle, two approaches are investigated. The first approach consists in forming a positive angle by adjusting the etching / passivation cycle steps when etching the silicon wafer from the front side (Figure 13 (a)). The backside is then etched by DRIE (Figure 12 and Figure 13 (a)). In the second approach, the silicon wafer is etched with a negative angle to obtain an underetched structure corresponding to the nozzle. (Figure 13 (b)). Then, still from the front side of the wafer, the wide opening is etched through another mask. Finally, the wafer is flipped to obtain the final structure as in Figure 12.

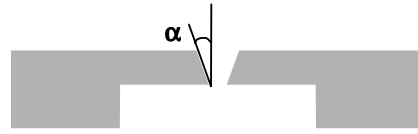


Figure 12: Schematic cross-section of a single nozzle.

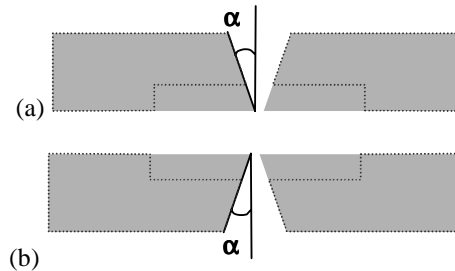


Figure 13: Nozzle diverging part fabrication (the final structure is outlined): (a) positive angle, (b) negative angle.

The first experiments have shown that no significant angle could be achieved with the first approach. It has not been possible to passivate sufficiently the sidewalls in order to reduce the etching surface at the bottom without stopping the etching. The second approach consisting in underetching the structure showed promising results. An angle of 3.7° had been obtained (Figure 14).

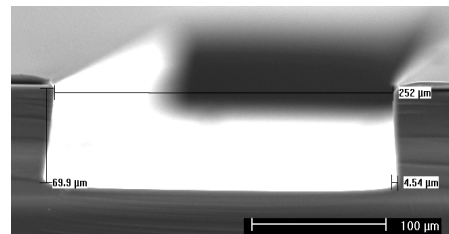


Figure 14: Negative angle of 3.7° etched by DRIE.

III.3 Fabrication of the chamber wafer

Two chamber materials have been considered to serve as propellant tank: silicon and Foturan, a photostructurable glass. On one hand, the main advantages of using silicon lie in its well-known technology fabrication and its high melting point. Moreover, the realisation of the micro-rockets parts using only silicon minimises the thermal expansion mismatch between the materials. On the other hand, Foturan offers a lower heat conductivity that can result in a better thermal insulation between the chambers, which could be of importance when considering the thermal cross-talk between a single rocket and its closest neighbours.

III.3.1 Silicon chambers

The silicon chambers were realized by deep reactive ion etching (DRIE) of silicon, using the Multiplex ICP (ASE HR) with the Bosch process [8] from Surface Technology Systems (STS). 525 μm - and 1 mm- thick wafers were etched through their whole thickness. A thick thermal oxide and a thick photoresist were used as mask. The chambers dimension is of $1.5 \times 1.5 \text{ mm}^2$ as stated in the section dealing with the design. However, smaller chambers of $500 \times 500 \mu\text{m}^2$ were also fabricated, this in order to build a more compact device (see section V). They could be surrounded by thermal insulating grooves if necessary, 50 μm - wide being the narrowest grooves that are achieved.

Due to the aspect ratio dependent etching rates of DRIE [9], a special mask design has been used to through-etch the narrow grooves without overetching the wide chambers. It consisted in etching the perimeter of the structures with a trench. When the etching reaches the bottom of the wafer, the chamber middle piece became separated from the bulk of the wafer, as illustrated in Figure 15. Since the trench width corresponded to the insulating grooves dimension, all structures were etched at the same rate and no significant overetching was noticed.

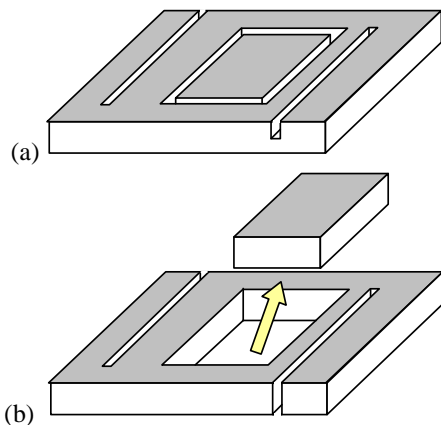


Figure 15: chambers and grooves etching principle: (a) grooves and chambers outline are etched, (b) the wafer is through-etched and the chamber middle piece comes off.

As shown in Figure 16 for 525 μm -thick wafers, the chambers and grooves exhibited a slightly bowed profile. At about 350 μm etch depth, the structures became 16 μm wider; the bottom was about 7 μm narrower than the top.

In the case of 1 mm- thick wafers, they were etched in two steps. A double side photolithography was used to pattern both the top and backside of the wafer.

First, the topside was etched up to about 575 μm deep. Then the wafer was turned over and the backside was etched through.

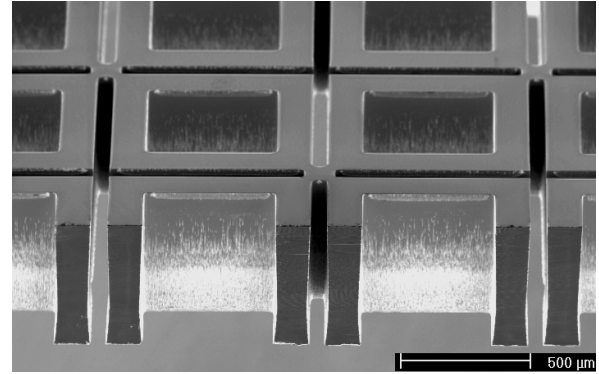
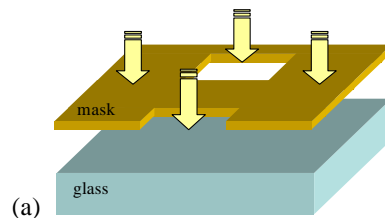


Figure 16: cross-section of $500 \times 500 \mu\text{m}^2$ chambers with 50 μm wide grooves etched by DRIE, Si wafer 525 μm - thick.

III.3.2 Foturan chambers

Foturan is a photoetchable glass from Schott that can be anisotropically wet etched. The Foturan wafers used were 1 mm- and 500 μm - thick, with chambers dimensions of $1.5 \times 1.5 \text{ mm}^2$. Firstly, the glass was exposed to UV light through a chromium mask in which the structures were drawn (Figure 17 (a)). Silver atoms were formed in the illuminated areas [10]. Then a heat development step was performed with temperature ramps up to 510°C and 595°C. During this heating step, the exposed glass crystallised around the silver atoms whereas the unexposed parts stayed in their glassy form (Figure 17 (b)). Finally, the etching was done in a 10% solution of hydrofluoric acid (HF) at room temperature using an ultrasonic bath (Figure 17 (c)). The exposed areas presented an etch rate about 20 times higher than that of the vitreous region. Since through-wafer holes were desired, the glass was etched from the top and backside at the same time.



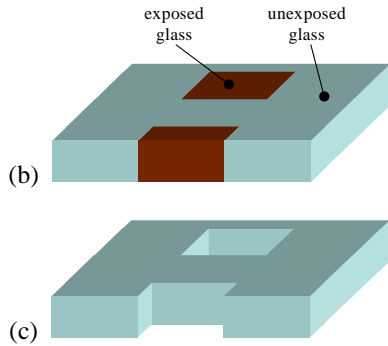


Figure 17: Foturan chambers process steps: (a) UV exposure, (b) heat development, (c) etching.

III.4 Wafer-to-wafer assembling

As shown in Figure 1, the micro-rocket array consists of a stack of 4 wafers. Because of the simplicity of the process and probable problems because of contamination after filling of the chambers with propellant, adhesive bonding was chosen for the assembling of the device. At first the nozzle part is bonded to the igniter part by a thermal epoxy (H 70 E, Polytec) and the seal wafer to the chamber wafer by a UV sensitive polymer (NOA 88, Norland) that can be spun-on the seal wafer. Since for the seal wafer Pyrex is used, the adhesive can be polymerized by UV-light. Then the igniter part is filled with the ignition propellant and the combustion chambers filled with the GAP based propellant. Finally the two wafer stacks are again bonded by thermal epoxy (H 70 E, Polytec). The annealing temperature of 60°C ensures that no ignition of the propellant occurs.

III.5 Packaging & electronic chip integration

The interconnection techniques and assembling procedures are strongly related to the electronic system architecture definition compatible with the microsystem assembling.

The final demonstrator will include in a minimum surface: Battery module, Power and multiplexing module, Control module and RF communication module (Figure 18).

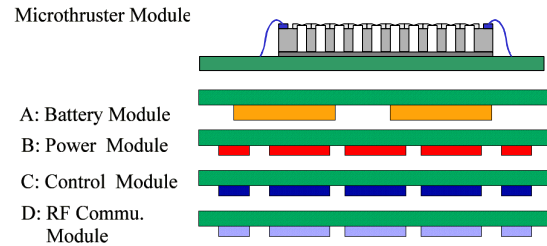


Figure 18: Final packaging and assembling process.

The specific electronic partition increases considerably the complexity of the final assembling process, increasing also parasitic effects. A better approach based on the global integration of all electronic circuitry in the same chip (System-on-Chip approach) is being evaluated.

IV. Micro-rockets testing

Two parameters are important to characterize our technology. The first one concerns the ignition process and the second concerns the combustion process and thrust generation.

IV.1 Ignition process

For ignition process, we used a Zirconium doped composite propellant. The filament is powered with an electrical current via a programmable power supply. When the ignition propellant is heated up at its ignition temperature, it burns leading to the rupture of the membrane and resistance. To determine the ignition energy, the time between the beginning of the ignition and the rupture of the membrane is measured.

Type of heater	Ignition power	Ignition energy	Percentage of ignition success
Heater #1 (540μm × 540μm)	225mW	105mJ	70%
Heater #2 (720μm × 720μm)	225mW	100mJ	

Table 2: Ignition characterization results.

IV.2 Combustion process and performance measurement

IV.2.1 Description of the thrust stand

The thrust stand used to characterize micro-rocket is schematically given in Figure 19 [11]. It consists of a thin and rigid arm (100 μm thick) rotating freely around a pivot. The rocket is mounted at the end of the arm. On the opposite face of the arm and aligned with the point of thrust application, a coil is deposited. The thrust stand is fixed on a marble block to minimize vibration disturbances during measurements.

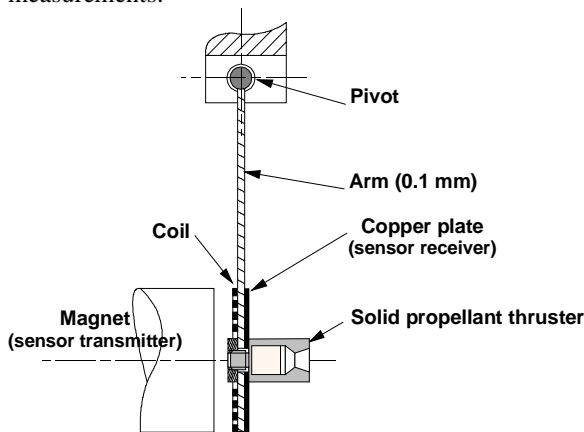


Figure 19: Schematic view of the thrust stand.

The coil is immersed in the magnetic induction field produced by the permanent magnet. When the thrust force is applied, the pendulum rotates around the pivot axis. A displacement sensor feeds a voltage to the electronic control, which increases the current in the coil and thus the restoring force until the reference position of the pendulum. The displacement sensor is a high frequency transmitter and an antenna, respectively a magnet and a copper plate. The distance between magnet and copper plate modulates the amplitude of the high frequency signal. A feedback control is obtained with a PID (Proportional Integral Derivative) circuit. Measurement of the equilibrium force equal to the thrust is obtained by measuring the electric current. For static calibration purposes, the pendulum is laid horizontally. Calibrated masses from 1 mg (10 μN) to 2 g (20 mN) are placed coincident with the thrust axis. The entire loop gain is 2.549 mN/V and sensitivity is 25 μN . To determine the natural frequency of the thrust stand, a force step is applied to the arm. The natural frequency of the system is 42 Hz. This stand has been used for measuring the thrust impulse and the combustion rate.

IV.2.2 First results

For thrust generation, a GAP based propellant is used. When the propellant is ignited at any point of its surface, the combustion occurs and propagates to all the surface and then progresses perpendicular to the combustion surface. The burning rate is thus defined by the change of thickness layer of burnt propellant as a function of time. Combustion tests have raised that the burning rate depends on the size of the combustion surface as well as on the environment. When the GAP propellant is loaded in a silicon chamber, its burn rate varies from 4.8mm/s and 5.3mm/s when the chamber section varies from 2.85mm² and 9.25mm². Below 1.9mm² (1.38mm \times 1.38mm), the combustion cannot be sustained for a Zr doped propellant. When the propellant is loaded in a glass chamber, the minimum section to have a sustained combustion decreases down to 1.8mm² (1.34mm \times 1.34mm). First thrust characteristics gave resulting impulse bit force of 6mN.s.

V. Towards a more compact rocket structure

With the aim of increasing the level of integration of the micro-rockets, a more compact device is under development. This is achieved by using a more energetic propellant stored in a smaller chamber. The chamber dimension would be reduced to a width of 250 to 500 μm . Moreover, the number of wafers that composes the structure of the rocket would be decreased using this design. This is obtained by integrating the igniter directly under the nozzle and the chamber and the seal together, as shown in Figure 20. The rocket would therefore consist of two wafers, the chamber and the igniter/nozzle. The chamber could be first filled with propellant and then closed by the igniter part having the nozzle integrated in it. In order to thermally isolate the heating resistors from the nozzle, the resistors would be suspended using surface micromachining.

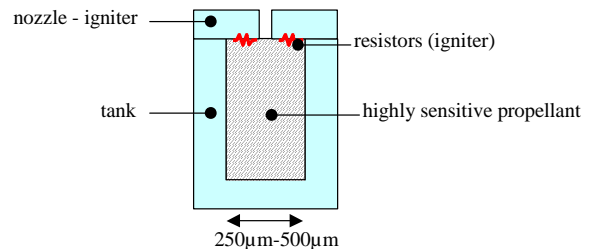


Figure 20: Schema of single more compact micro-rocket.

VI. Summary

In this paper, we reported on an array of micro-rockets on silicon. The paper described the design and initial results obtained for the fabrication, assembling and testing of the devices. The work described has been performed within an EC funded project (IST-99047) [12]. Partners are LAAS (CNRS laboratory-France), IMT (University of Neuchâtel-Switzerland), IMTEK (University of Freiburg-Germany), SIC (University of Barcelona-Spain), ASTC (University of Uppsala-Sweden), LACROIX (France).

In conclusions :

- Some micro-rocket samples have been successfully tested with solid propellant.
- Flexible 2D addressing design has been realized.
- Study of epoxy and UV gluing has been performed.
- Even if one design has been presented in this paper, the structure is flexible and can incorporate different heater sizes, different chamber lateral dimensions. Different propellant material have been formulated and tested. Characterizations showed that propellant studied can not have reproducible sustained combustion down to the millimeter scale chamber. A thrust stand has been built and will be used for the ground testing of the micro-rockets array.

Integration issue being one important point for MEMS : new type of igniter and new energetic material as presented in § V are under investigation.

One entire addressed matrix of micro-rockets will be assembled and characterized by the end 2002.

VII. References

- [1] I.A. Waitz et al, Combustors for Micro-gas turbine engines, ASME, J. of Fluids Eng. , March 1998, vol 120
- [2] A.P. London et al, Microfabrication of a high pressure bipropellant rocket engine, A, 92 (2001), 351-357
- [3] W. Lindsay et al, Thrust and Electrical Power from Solid Propellant Microrockets, 14th IEEE International Conference on Micro Electro Mechanical Systems, Piscataway, NJ, USA, 2001, pp606-10
- [4] Mehra. A et al, A six-wafer combustion system for a silicon micro gas turbine engine, Journal of Micro Electro Mechanical Systems, Vol.9, N4, Dec 2000, pp517-527
- [5] C. Rossi, Evaluation of Solid Propellant Technology for Small Satellite Station Keeping, Rapport LAAS N° Rapport contrat ESA
- [6] E.B. Rudnyi, T. Bechtold, J. Korvink, C. Rossi, bSolid Propellant Microthruster : Theory of Operation and Modelling Strategy, NanoTech conference, Houston, September 2002
- [7] Miribel, P.; Montané, E.; Puig-Vidal, M.; Samitier, J.; "A Buck DC/DC synchronous converter applied to micro-ignition systems" DCIS 2002 International Conference of Design Circuits and Systems. November 2002
- [8] F. Lärmer and A. Schilp, Robert Bosch GmbH, *Method of Anisotropically Etching Silicon*, Pat. 4241045C1 (DE), 4855017 and 4784720 (USA)
- [9] J. Kiihamäki and S. Franssila, *Pattern shape effects and artefacts in deep silicon etching*, J. Vac. Sci. Technol. A 17 (4) (1999) 2280-2285
- [10] mgt mikroglas technik AG, <http://www.mikroglas.com>
- [11] S. Orioux, C. Rossi, D. Estève, Thrust stand for ground tests of Solid Propellant Microthrusters Review of Scientific Instruments, Vol. 73, Number 7, July 2002
- [12] <http://www.laas.fr/~micropyros>